RSC Advances

PAPER

View Article Online
View Journal | View Issue

Cite this: *RSC Adv.*, 2022, **12**, 13235

Preparation of a quartz microbalance sensor based on molecularly imprinted polymers and its application in formaldehyde detection

Junbo Liu,[a] Wensi Zhao,[b] Jin Liu,[a] Xuhong Cai,[a] Dadong Liang,*[a] Shanshan Tang *[a] and Bao Xu[c]

Quartz crystal microbalances (QCMs) have been widely used in the food industry, environmental monitoring, and biomedicine. Here, a molecularly imprinted QCM sensor was prepared and used for formaldehyde detection. Using polyvinyl chloride as the embedding material and tetrahydrofuran as the solvent, a QCM electrode was modified with HCHO molecularly imprinted polymers (HCHO-MIPs). The detection conditions of the sensor were optimized, and its selectivity was investigated. The theoretical calculation results revealed that the acrylamide and pentaerythritol triacrylate were potential candidate functional monomer and cross-linking agent, respectively, in the preparation of HCHO-MIPs with high adsorbability, superselectivity, and stability. According to the calculated results, a sensor had been prepared. When the pH was 7, the added mass of the HCHO-MIPs (or NIPs) was 20 mg, and the amount of PVC coating was 20 μL, the sensor exhibited good adsorption, selectivity, repeatability, high sensitivity, high accuracy, and a short response time. The lowest detection limit was 10.72 ng mL^{-1}. The sensor exhibited higher selectivity for HCHO than for propionaldehyde and benzaldehyde. The HCHO contents in fresh shrimp samples were detected using the sensor for four cycles, and the detection rates were in the range of 97.56–98.60%. This study provided a theoretical and experimental basis for the rapid detection of HCHO.

Received 16th March 2022
Accepted 27th April 2022

DOI: 10.1039/d2ra01705a

rsc.li/rsc-advances

Introduction

Formaldehyde (HCHO) has an irritating odour and is biologically toxic. It can damage human cell functions, mainly manifesting in irritation, allergies, and abnormal liver function, lung function, and immune function. In addition, it exhibits a strong carcinogenic effect.[1] HCHO has been exploited as a preservative for vegetables, fresh fish, shrimp, and other products because of its bactericidal and anticorrosive effects[2] and is a threat to human health. Therefore, establishing a fast, sensitive, and accurate detection technology for low-concentration HCHO samples is a key topic in environmental chemical pollutant detection.

Presently, the main detection methods for environmental HCHO pollutants include chromatography,[3,4] spectrophotometry,[5,6] infrared spectroscopy,[7–9] polarography, and electrochemical detection.[10–12] However, owing to its low concentration and ease of coexisting with other pollutants, HCHO pollutant samples typically require pretreatment before detection to achieve enrichment and separation. Presently, the interaction between the conventional solid-phase extraction adsorbents (C8, C18, diatomite, and silica gel) and analyte is non-specific. Thus, many components in the sample matrix are simultaneously extracted. It is easy to introduce errors, and the extraction column can only be used once, which leads to poor reproducibility. In addition, for all the detection methods, samples need to be collected at the monitoring site and analysed in the laboratory. The traditional analysis method involves a long cycle, high cost, and complicated steps.

In 1880, the Curie brothers first discovered the piezoelectric effect,[13] which is that two ends of a crystal can produce different charges when an external force is applied to a quartz crystal (QC) wafer in a certain direction. Contrarily, the QC wafer oscillates periodically when an electric field is applied to both the ends of the crystal; this is the inverse piezoelectric effect. This effect was used for the first time in a QC microbalance (QCM) sensor. It is a sensitive instrument that can detect changes in nano mass. The quality change in the electrode surface can change the vibration frequency of the QC wafer. Thus, the QCM sensor can be used to analyse and detect trace substances. It was first used in meteorological research.[14] Subsequently, the invention of the high-gain oscillation ring

[a]College of Resources and Environment, Key Laboratory of Straw Biology and Utilization, Ministry of Education, Jilin Agricultural University, Changchun 130118, China. E-mail: liangdadong@jlau.edu.cn

[b]State Key Laboratory of Environmental Criteria and Risk Assessment, Chinese Research Academy of Environmental Sciences, Beijing, China

[c]Institute of Mathematica, Jilin Normal University, Siping, Jilin 136000, China

greatly promoted the development of QCM in the liquid phase.[15]

In comparison with other analyses, the use of QCM can realise real-time *in situ* monitoring of reaction progress. Moreover, owing to its simple construction, rapid response, high sensitivity, easy operation, and short detection time, QCM has been widely used in biology analysis.[16] The specific process of reactions can be expounded using dynamic parameters obtained by real-time monitoring. It can provide important evidence to distinguish specific and non-specific reactions. QCM has been widely used in biomedicine, pharmaceuticals, and food[17–20] since the 1990s. To obtain better selectivity, molecularly imprinted polymers (MIPs) can be used as the recognition component of the QCM sensor. It can be fixed on the electrode surface of the QCM sensor to construct a MIPs-QCM sensor. When the MIPs were used as the sensitive identification component, owing to its specific adsorption of the target material, the sensor exhibited good selectivity, strong anti-interference ability, and high accuracy. Recently, MIPs have been combined with QCM to determine many molecules, such as copper aldehydes,[21] acrylamides,[22] L-tryptophan,[23] and cystine bridging cyclic peptide hormones.[24] However, there were very few researches referred to MIPs-QCM for testing HCHO.[25,26]

Here, the optimized functional monomers and cross-linking agents (CLAs) were used to prepare HCHO-MIPs. The HCHO-MIPs were coated on the QCM electrode to construct an HCHO-MIPs-QCM sensor to detect HCHO. This sensor was used to detect HCHO in fresh shrimp samples.

Calculations

The geometric configurations of HCHO, itaconic acid (IA), acrylamide (AM), and 4-vinylpyridine (4-VPY) were optimised using the B3LYP method and the 6-31G(d,p) basis set.[27] The counterpoise (CP) method was used to eliminate the basis set superposition error of the HCHO–AM (IA, 4-VPY) complex. The calculation equation is as follows:

$$\Delta E_{CP} = E_T - E_{HCHO} - \sum E_F, \quad (1)$$

ΔE_{CP} (kJ mol^{-1}), E_{HCHO} (kJ mol^{-1}), and $\sum E_F$ (kJ mol^{-1}) are the binding energy of the stable complex corrected using the CP method, energy of HCHO and sum energy of the functional monomer, respectively. E_T (kJ mol^{-1}) represents the total energy of the stable complex formed from the functional monomer and corrected HCHO.

The binding energy between AM and four CLAs was calculated using the equation:

$$\Delta E_1 = E_E - E_{CA} - E_F, \quad (2)$$

ΔE_1 (kJ mol^{-1}) represents the binding energy of the stable complex modified using the CP method. E_E (kJ mol^{-1}) is the total energy of the stable complex formed from a CLA and AM. E_{CA} (kJ mol^{-1}) and E_F (kJ mol^{-1}) are the energies of the CLA and functional monomer, respectively.

Experiments

Reagents and equipment

HCHO, propionaldehyde, benzaldehyde, and pentaerythritol triacrylate (PETA) were purchased from Shanghai Aladdin Reagent Co., Ltd. AM was purchased from Sinopharm Chemical Co., Ltd. Azobisisobutyronitrile, methanol, tetrahydrofuran, and acetic acid were purchased at the Beijing Chemical Plant. Polyvinyl chloride (PVC, S-1000) was purchased from the China Petrochemical Corporation, Qilu Branch. All the reagents were analytical pure.

An ultraviolet-visible spectrophotometer (TU-1901) was purchased from Beijing Puji General Instrument Co., Ltd. A QCM analyser (CHI400C) was purchased from Shanghai Chenhua Instrument Co., Ltd.

Preparation of HCHO-MIPs

Initially, 2 mmol of HCHO was dissolved in 50 mL of the methanol solvent. AM and PETA were added in at a molar ratio of 1 : 4 : 16 for HCHO, AM, and PETA. The initiator (azobisisobutyronitrile) was added and sonicated for 0.5 h. After nitrogen had been aerated for 5 min, the thermal polymerisation reaction was performed for 48 h in a water bath at 323 K. After the precipitated polymer was obtained, it was dried in a vacuum drying oven. Thereafter, the acetic acid and methanol elution solution with a volume ratio of 3 : 7 was used for soxhlet extraction to completely remove the HCHO of the polymer. The polymer was washed with methanol to remove the residual acetic acid. Finally, the HCHO-MIPs were dried in a drying oven. The preparation process of non-molecular imprinted polymers (NIPs) was the same as that of HCHO-MIPs, except that the HCHO was not added.

Sensor response research

The piezoelectric QC electrode (AT section, gold/chrome polishing) has a fundamental frequency of approximately 8 MHz and a diameter of 10 mm. The relationship between the change in the QC loading and the change in substrate frequency was used to detect the measured material. The formula is as follows:

$$\Delta f = f_i - f_0, \quad (3)$$

$$\Delta f = -2.26 \times 10^{-6} f_0^2 \Delta m / A, \quad (4)$$

Δf (Hz) is the frequency change value of the QC, f_i (Hz) is the response frequency of the electrode, f_0 (Hz) is the basic resonant frequency of the electrode, Δm (g) is the total mass of the MIPs (or NIPs) to HCHO and A is the dial area (0.205 cm^2) across the crystal.

The modified QCM electrode was fixed in the detection cell. Thereafter, 2 mL of a phosphate buffer (PB) solution was added as the background solution, and the electrolytic cell was connected. When the frequency change was not over 20 Hz and was in a stable state, the reference frequency of detection was f_0. Afterwards, 20 μL of the HCHO solution was quickly added to the detection pool, and the response frequency, f_i, was recorded

for 30 min. The frequency change value, Δf, was calculated according to eqn (3), and the binding amount, Δm, of the MIP (NIP)-modified membrane to HCHO was calculated using eqn (4).

After recording, the electrode was removed, and its modified film was eluted with the elution solution. The modified film electrode was rinsed with distilled water. The cleaning step was repeated for five times. When the detected response frequency of the modified film was the reference frequency, it indicated that the modified film had been eluted. Then the modified film was stored in the drying oven for future use.

Electrode modification of molecularly imprinted QCM sensor

Pretreatment of the electrode. The electrode substrate was immersed in a piranha solution with a 1 : 3 volume ratio of H_2O_2 to H_2SO_4 for 5 min. The surface of the electrode was washed with ultrapure water. The aforementioned steps were repeated for five times. Finally, the surface of the substrate was dried with nitrogen after being washed with ultrapure water. The samples were stored in the drying oven for future use.

Electrode modification. Here, 20 mg of HCHO-MIPs (or NIPs) was placed in 10 mL of tetrahydrofuran under ultrasonic oscillation for 30 min. Thereafter, 20 mg of PVC was added. The modified electrode of the HCHO-MIPs (or NIPs) was obtained after the tetrahydrofuran was volatilised. The modified electrode was stored in the drying oven for future use.

Optimisation of detection conditions

When the molecularly imprinted QCM sensor was constructed, the adding dosage of the polymer, dosage of the coating film, and pH may affect the response frequency of the HCHO. Here, the effects of the different MIP and NIP dosages (10.0, 20.0, and 30.0 mg), dosages of the coating film (5, 10, 15, 20, and 25 μL), and pH levels (3, 5, 7, 9, and 12) on the response frequency of the sensor were investigated.

Selectivity study of sensors

Under the optimized condition, the response values of HCHO and its analogues (benzaldehyde and propionaldehyde) in a methanol solution were detected using the HCHO-MIPs sensor for evaluating its selectivity. The concentration of the standard solution was 200 ng mL^{-1} for HCHO, benzaldehyde and propionaldehyde in methanol. Moreover, the selectivity coefficient (α) was calculated. The formula is as follows:

$$\alpha = \Delta F_{HCHO}/\Delta F_I, \quad (5)$$

ΔF_{HCHO} (Hz) is the response frequency of sensor to HCHO, ΔF_I (Hz) means the response frequency of sensor to analogues (benzaldehyde and propionaldehyde) of HCHO.

Detection application of sensor in fresh shrimp samples

Sample pretreatment. Here, 1.00 g of fresh shrimp was pounded and placed in a 15 mL centrifuge tube. Thereafter, 1.0 mL of the HCHO standard solution with a concentration of 200 ng mL^{-1} was added into the tube (1.0 mL of methanol was added to the blank control group). Afterwards, 9 mL of methanol was added into both samples. After ultrasonic treatment for 10 min, the samples were centrifuged for 20 min at 5000 rpm. The supernatant was dissolved with methanol to a constant volume of 10 mL. The samples were stored for the subsequent application.

Sample detection. 20 μL of the sample solution was added to the background solution, and the response values were recorded after the QCM sensor was switched on. The methanol/acetic acid solution (9/1, v/v) was used to elute HCHO (substrate), which was combined with the modified film. The substrate was washed for several times with ultrapure water until the stable frequency of f_0 was detected in the background solution. The surface of the electrode was blow-dried with nitrogen and placed on standby for subsequent application.

Results and discussion

Functional monomer optimisation

The structural and functional groups of imprinted molecules mainly determine the selection of functional monomers. The complex formed from imprinted molecules and functional monomers is the basis for forming memory recognition sites for MIPs. When the complex had a high imprinted ratio, large number of hydrogen bonds, and low binding energy, the MIPs would possess numerous bonding sites. Additionally, it would exhibit high stability, better adsorption and selectivity properties. Therefore, screening the functional monomers to match the space configuration of imprinted molecules is significant.

At the B3LYP/6-31G(d,p) level, the stable configurations of the stable complexes with the optimal molar ratios between HCHO and different functional monomers (IA, AM, and 4-VPY) were simulated, and the results are shown in Fig. 1. The action site, molar ratio, hydrogen bond length, and binding energy between HCHO and the functional monomer of each stable complex were shown in Table 1. As observed in Fig. 1 and Table 1, the molar ratios of the complexes formed from HCHO and different functional monomers (IA, AM, and 4-VPY) are 1 : 3, 1 : 4, and 1 : 1, respectively. The numbers of their hydrogen bonds are 5, 5, and 1, respectively. Their binding energies are −71.16, −109.51, and −33.50 kJ mol^{-1}, respectively. The hydrogen bond lengths are in the range of 0.1797–0.2415 nm for

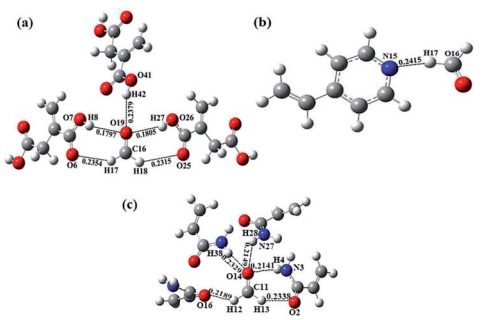

Fig. 1 Optimal stable complex configurations of (a) HCHO and IA, (b) 4-VPY (c) AM functional monomers.

Table 1 The relevant parameters of the stable complexes formed from HCHO and IA, AM and 4-VPY, respectively

Complex	Action site	*R*/nm	Imprinted ratio	Hydrogen bonds	ΔECP (kJ mol^{-1})
HCHO–IA	C16–H17···O6	0.2354	1 : 3	5	−71.16
	C16–H18···O25	0.2315			
	O7–H8···O19	0.1797			
	O26–H27···O19	0.1805			
	O41–H42···O19	0.2379			
HCHO–4-VPY	C16–H17···N15	0.2415	1 : 1	1	−33.50
HCHO–AM	C11–H12···O16	0.2189	1 : 4	5	−109.51
	C11–H13···O2	0.2338			
	N37–H38···O14	0.2329			
	N3–H4···O14	0.2141			
	N27–H28···O14	0.2149			

all interaction ratios, and they are within the category of hydrogen bond lengths.[28] The molar ratio of the HCHO–AM complex is larger than those of the HCHO–IA and HCHO–4-VPY complexes, while the binding energy is considerably smaller than those of the HCHO–IA and HCHO–4-VPY stable complexes. Thus, AM is a potential candidate to prepare HCHO-MIPs with high adsorbability, superselectivity, and stability.

CLA optimisation

CLAs can fix the functional group of a monomer to a specific position around the stereoscopic pores of the MIPs. The performance of a CLA is an important factor that affects the specific adsorption and stability of HCHO-MIPs. To improve the imprinting efficiency of the HCHO-MIPs, the binding energy between the selected CLA and functional monomer should be low. Therefore, the polymer will have holes in a certain spatial configuration. Simultaneously, the functional residues derived from AM can be orderly arranged in the stereoscopic holes of highly cross-linked HCHO-MIPs. The binding energies between AM and divinylbenzene (DVB), ethylene glycol dimethylacrylate (EGDMA), PETA, and trimethacrylate (TRIM) (reaction ratio is 1 : 1) were listed in Fig. 2. As shown in Fig. 2, the order of the binding energy between AM and the CLAs is PETA < EGDMA < TRIM < DVB. The binding energy between AM and PETA is the lowest among the selected CLAs. Thus, PETA is more suitable as a CLA to prepare the HCHO-MIPs than the other three CLAs (DVB, EGDMA, and PETA).

Influence of polymer addition quality on sensor response frequency

When the pH of the PB background solution was 7 and the PVC coating amount was 20 μL, the HCHO-MIPs (NIPs) microspheres with different masses were fixed onto the electrode surface using the PVC embedding method. Then the stabilised frequency was recorded, and the results were shown in Fig. 3. When the HCHO-MIPs (or NIPs) was not added, there was no imprinted or non-imprinted binding site on the modified film, and the sensor response was extremely weak. When the mass of the HCHO-MIPs (or NIPs) increased, the imprinted or non-imprinted binding sites on the modified film increased, and the response frequency of the sensor gradually increased. When 20.0 mg of the MIPs (or NIPs) was added, the response frequency of the sensor reached its maximum. When the mass of the HCHO-MIPs (or NIPs) increased to 30.0 mg, the response frequency of the sensor decreased. This might be because the excess imprinted binding sites (HCHO-MIPs) or non-imprinted binding sites (or NIPs) of the modified film on the electrode generated accumulation, which resulted in the weak response of the sensor.

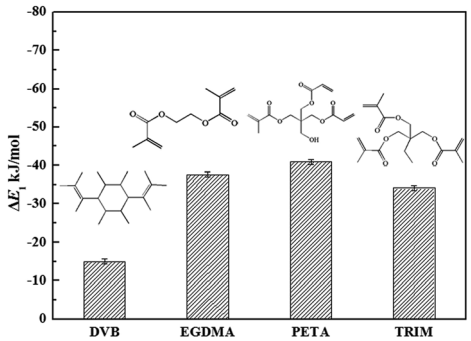

Fig. 2 Binding energy (ΔE_1) between AM and the cross-linking agents.

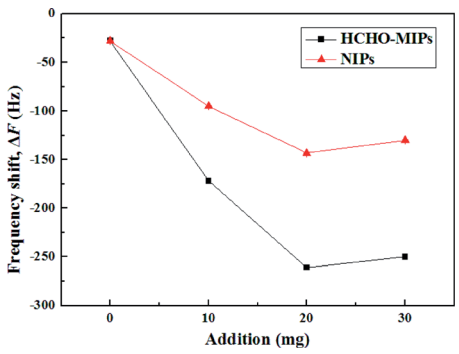

Fig. 3 Frequency shift with the different additions for the HCHO-MIPs and NIPs.

Compared with the HCHO-MIPs, the response of the NIP-modified sensor is weak because there is no specific binding site for HCHO in the NIP-modified film. The NIP-modified film only provides non-specific physical adsorption for HCHO. Thus, the response of the sensor with the NIP-modified film is weak. Therefore, when the mass of the HCHO-MIPs was 20 mg, the sensor had the best response effect.

Influence of PVC coating amount on sensor response frequency

When the pH of the PB background solution was 7 and the mass of the HCHO-MIPs was 20 mg, the effects of different PVC coating amounts (5, 10, 15, 20, and 25 μL) of the electrode on the frequency response to HCHO were investigated. As shown in Fig. 4, as the amount of coating increased, the response frequency of the sensor continuously increased. When the amount of coating was 20 μL, the response frequency of the sensor reached its maximum. When the coating volume increased to 25 μL, the response frequency of the sensor slightly decreased. This may be because the modified film was extremely thick, and the MIPs on the film were densely distributed or stacked. Thus, the amount of adsorbed HCHO may be reduced, which weakened the response of the sensor.

The influence of pH of PB background solution on sensor response frequency

The response frequency of the QCM sensor to HCHO was detected in the PB background solution at different pH levels (3, 5, 7, 9, and 12). As shown in Fig. 5, the response frequency of sensor to HCHO was the highest when the pH was 7. This may be because the interaction between the determinant and HCHO-MIPs of the sensor was mainly through hydrogen bonds. When the pH of the solution was lower than 7, the aldehyde group of HCHO would be protonated. It weakened the nucleophilicity of the oxygen atoms in HCHO. When the pH of the solution exceeded 7, HCHO would lose protons. As a result, the hydrogen bond interaction between the HCHO and action sites of the HCHO-MIPs became weak in both acidic and alkaline solutions, which reduced the adsorption capacity. The change in pH slightly affected the response of the NIP sensor. No template molecule was added during the synthesis of NIPs; therefore, the binding site of NIPs was reduced.

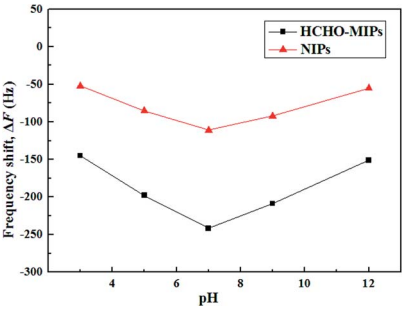

Fig. 5 Effect of pH levels on the response frequency of the sensor.

Response characteristics of sensors

When the pH of the PB background solution was 7, the mass of HCHO-MIPs was 20 mg, and coating amount of PVC was 20 μL, the response frequencies of the sensor for HCHO solutions at different concentrations were investigated (Fig. 6). As shown in Fig. 6, as the concentration of the HCHO solution increased, the response frequency of the sensor gradually increased. The frequency change of the HCHO-MIP-modified electrode was larger than that of the NIP-modified electrode, and the difference increased with an increase in the concentration. In addition, the response regression equation of the HCHO-MIP-modified sensor in the detection concentration range was $Y = -1.156X - 35.561$ ($R^2 = 0.9999$). According to the equation, the limit of detection (LOD) was $3.3\delta/S$ (S, slope; δ, residual standard deviation); the LOD of the HCHO-MIP-modified sensor was 10.72 ng mL^{-1}.

Selective study of sensors

To investigate the selectivity of the HCHO-MIP-modified QCM sensor, the response frequencies of HCHO and its structural analogues (propionaldehyde and benzaldehyde) were measured (Fig. 7). The response frequency order of the QCM sensor to HCHO and its structural analogues is HCHO > propionaldehyde > benzaldehyde. The selective recognition of the QCM sensor to

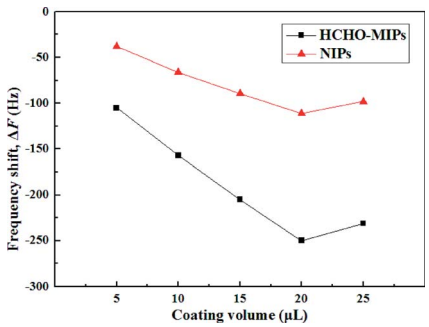

Fig. 4 Variation in the sensor response frequency with different coating amounts.

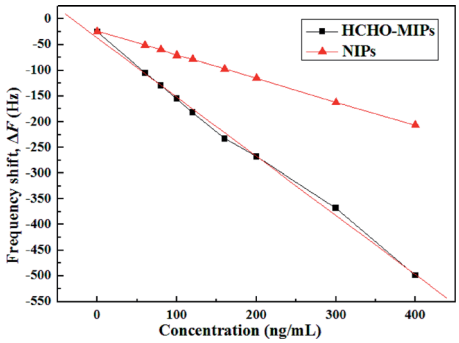

Fig. 6 Response frequency of the sensor for the HCHO solutions at different.

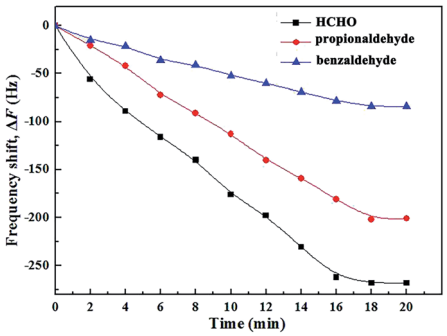

Fig. 7 Sensor selectivity for HCHO, propionaldehyde and benzaldehyde.

HCHO is the best. This may be because the size and shape of the HCHO-MIP holes and their residual functional groups were highly matched with HCHO imprinted molecules. The electrodes modified by the structural analogues of HCHO also exhibited a certain response to HCHO. Moreover, the response strength of propionaldehyde is larger than that of benzaldehyde because benzaldehyde contains a benzene ring, which is considerably different from the structure of HCHO. When the reacted time reached 18 minutes, the response value (−268 Hz) of the sensor to HCHO was the largest. According to the formula (5), the α values of sensor to benzaldehyde and propionaldehyde were 3.19 and 1.33, respectively. It reveals that the sensor has strong selectivity to HCHO when it coexists with benzaldehyde and propionaldehyde. Summarily, the HCHO-MIP-modified QCM sensor has good selective recognition ability to HCHO.

Detection application of sensor in fresh shrimp sample

Table 2 shows the detection rates of the HCHO-MIP-modified electrode. As shown, the detected response value of the sample was −268 Hz after the first cycle with a corresponding concentration of HCHO in the sample at 197.21 ng mL^{-1}. With an increase in the number of cycles, the response value of the sensor to HCHO in the sample slightly decreased. After four cycles, the response value of the sensor to HCHO was −251 Hz, and the corresponding concentration of HCHO in the sample is 195.11 ng mL^{-1}. Additionally, the detection rate (97.56%) of the HCHO-MIP-modified electrode remains at an acceptable level. Moreover, when the QCM sensor was used for 7 times, the corresponding concentration of HCHO in the sample reached 188.50 ng mL^{-1}. Compared with the original concentration (200.00 ng mL^{-1}), it had only a 5.75% reduction. Thus, the sensor may be used for HCHO detection in food samples.

Table 2 The cycling performance of the sensor tested in the samples

Times	Response values (Hz)	Concentrations (ng mL^{-1})	Detection rates (%)
1	−268	197.21	98.60
2	−264	196.12	98.06
3	−257	195.87	97.94
4	−251	195.11	97.56

However, the surface of HCHO-MIPS modified electrode will be damaged more or less during the cleaning processes. Thus, the response frequency stability of the constructed QCM sensor decreased significantly after being continuously used for 7 times. It will increase the error of detection results.

Conclusions

Here, a novel HCHO molecularly imprinted QCM sensor was prepared by embedding it with an HCHO-MIP-modified QCM electrode. The results showed that the response frequency of the HCHO molecularly imprinted QCM sensor reached its maximum when the pH of the PB background solution was 7, the added mass of the HCHO-MIPs (or NIPs) was 20 mg, and the amount of PVC coating was 20 μL. Under the optimal conditions, the regression equation $Y = -1.156x - 35.561$ ($R^2 = 0.9999$) was obtained for the HCHO solution of different concentrations (60–400 ng mL^{-1}), and the minimum LOD was 10.72 ng mL^{-1}. Moreover, the HCHO content in fresh shrimp samples was detected using the sensor after four cycles, and its detection rate was in the range of 97.56–98.60%. This study provided theoretical and experimental references for the detection of HCHO in samples using the HCHO molecularly imprinted QCM sensor.

Author contributions

Junbo Liu: conceived and designed the experiments, funding acquisition. Wensi Zhao: performed the experiments, writing – original draft. Jin Liu, and Xuhong Cai: analyzed the data and drew the pictures. Dadong Liang: analyzed the data and modified the original draft. Shanshan Tang: conceived and designed the experiments, writing – original draft. Bao Xu: provided the software.

Conflicts of interest

There are no conflicts to declare.

Acknowledgements

The Science and Technology Development Planning of Jilin Province (20200201202JC).

Notes and references

1 M. Jalali, S. R. Moghadam, M. Baziar, G. Hesam and H. R. Zakeri, *Environ. Sci. Pollut. Res.*, 2021, **28**, 2.
2 A. Kundu, P. Dey, R. Bera, R. Sarkar and H. S. Kim, *Environ. Sci. Pollut. Res.*, 2020, **27**, 14.
3 S. Kim and H. J. Kim, *Bioresour. Technol.*, 2005, **96**, 1457–1464.
4 N. Kobayashi, T. Suzuki, Y. Kosugi, M. Hishiki, Y. Kado, S. Kaneta, H. Ueda, N. Kawai, Y. Kitamoto and K. Tsuchiya, *J. Jpn. Soc. Water Environ.*, 2016, **39**, 211–224.
5 M. Q. Wang, *Quality and Technical Supervision Research*, 2019, **96**, 47–50.

6 L. Teixeira, O. E. S. Le, A. F. Dantas, L. C. Pinheiro Helosa, A. C. S. Costa and J. B. D. Andrade, *Talanta*, 2004, **64**, 711–715.
7 K. Tanaka, S. Sugano, H. Nagata, S. Sakaida and M. Konno, *Appl. Phys. B*, 2019, **125**, 1–9.
8 J. Ghosh, G. Vishwakarma, S. Das and T. Pradeep, *J. Phys. Chem. C*, 2021, **125**, 4532–4539.
9 R. Zhu, R. Chen, Y. Duo, S. Zhang, D. Xie and Y. Mei, *Polymers*, 2019, **11**, 86–99.
10 R. B. Zhang, J. Hao, L. P. He and J. Shen, *J. Environ. Health*, 2005, **22**, 140–141.
11 D. D. Yuan, L. Tian, D. Gu, X. Y. Shen, L. Y. Zhu, H. J. Wu and B. H. Wang, *J. Cleaner Prod.*, 2017, **156**, 310–316.
12 A. Fornazari, G. Malpass, D. W. Miwa and A. J. Motheo, *Water, Air, Soil Pollut.*, 2012, **223**, 4895–4904.
13 J. Valasek, *Phys. Rev.*, 1920, **17**, 475–481.
14 W. H. King, *Anal. Chem.*, 1964, **36**, 1735–1739.
15 T. Nomura and M. Okuhara, *Anal. Chim. Acta*, 1982, **142**, 281–284.
16 E. Haghighi and S. Zeinali, *RSC Adv.*, 2019, **9**, 24460–24470.
17 E. Haghighi and S. Zeinali, *RSC Adv.*, 2019, **9**, 24460–24470.
18 H. Yang, Y. Li, D. Wang, Y. Liu, W. Wei, Y. Zhang, S. Liu and P. Li, *Chem. Commun.*, 2019, **55**, 9857.
19 G. Guerra, P. Arpaia, R. S. L. Moriello and G. Mensitieri, *IEEE Trans. Instrum. Meas.*, 2005, **54**, 31–37.
20 C. I. Cheng, Y. P. Chang and Y. H. Chu, *Chem. Soc. Rev.*, 2012, **41**, 1947–1971.
21 S. K. Jha and K. Hayashi, *Sens. Actuators, B*, 2015, **206**, 471–487.
22 H. F. El-Sharif, H. Aizawa and S. M. Reddy, *Sens. Actuators, B*, 2015, **206**, 239–245.
23 F. Liu, L. Xiao, S. C. Ng and S. O. Chan, *Sens. Actuators, B*, 2006, **113**, 234–240.
24 C. Lin, S. Tsai and D. Tai, *J. Pept. Sci.*, 2019, **25**, 1–8.
25 M. Hussain, K. kotova and P. A. Lieberzeit, *Sensors*, 2016, **16**, 1011–1013.
26 S. Carquigny, N. Redon, H. Plaisance and S. Reynaud, *IEEE Sens. J.*, 2012, **12**, 1300–1306.
27 W. S. Zhao, J. B. Liu, S. S. Tang and R. F. Jin, *J. Mol. Model.*, 2020, **26**, 88–95.
28 B. G. Oliveira, F. S. Pereira, R. C. M. U. D. Araújo and M. N. Ramos, *Chem. Phys. Lett.*, 2006, **427**, 181–184.